A Novel ^{18}F-Labeled Imidazo[2,1-b]benzothiazole (IBT) for High-Contrast PET Imaging of β-Amyloid Plaques

Behrooz H. Yousefi,[*,†] Alexander Drzezga,[†] Boris von Reutern,[†] André Manook,[†] Markus Schwaiger,[†] Hans-Jürgen Wester,[‡] and Gjermund Henriksen[*,†]

[†]Department of Nuclear Medicine, Klinikum rechts der Isar, Technische Universität München, Ismaninger Strasse 22, 81675 München, Germany

[‡]Lehrstuhl für Pharmazeutische Radiochemie, Walther-Meissner-Strasse 3, 85748 Garching, Germany

S *Supporting Information*

ABSTRACT: ^{18}F-labeled imidazo[2,1-b]benzothiazole ([^{18}F]8) was synthesized and evaluated as a tracer for cerebral β-amyloid deposits (Aβ) by means of positron emission tomography (PET). [^{18}F]8 exhibits a high affinity to Aβ and suitable brain uptake kinetics combined with a high metabolic stability in the brain. In a double transgenic APP/PS1 mouse model of Alzheimer's disease, we demonstrated a specific uptake of [^{18}F]8 in Aβ-containing telencephalic brain regions. The specific binding of [^{18}F]8 to Aβ was confirmed by regional brain biodistribution and autoradiography and correlated to immunohistochemistry staining. Analysis of brain sections of APP/PS1 mouse injected with a cocktail of [^{18}F]8 and reference compound [^{3}H]PiB revealed that the two tracers bind to Aβ plaques in the brain of mouse in a comparable binding pattern. [^{18}F]8 represents the first high-contrast PET imaging agent for detection of Aβ plaques in transgenic mouse model of Alzheimer's disease and holds promise for transfer to a clinical evaluation.

KEYWORDS: Alzheimer's disease, ^{18}F-labeled tracer for β-amyloid, IBT, β-amyloid plaques, positron emission tomography, autoradiography, APP/PS1transgenic mice, neuroimaging
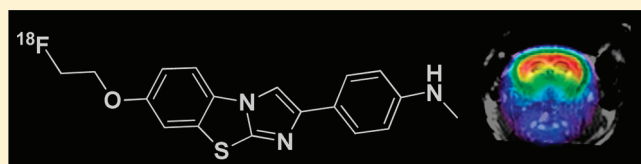
Current tracer development for the noninvasive imaging of Alzheimer's disease (AD) is focused on markers of senile plaques (SP) that consist of β-amyloid peptides (Aβ) with positron emission tomography (PET).[1−4] Several [11]C- and ^{18}F-labeled PET tracers have been provided, including (N-[^{11}C-methyl])-6-OH-BTA-1, Pittsburgh compound B ([^{11}C]PiB, **1a**),[5] its ^{18}F-labeled analogue derivative 3′-[^{18}F]FPiB (Flutemetamol, GE-067, **1b**),[6,7] [^{11}C]SB-13 (**1c**),[8] [^{18}F]Florbetaben (**1d**),[9,10] [^{18}F]-Florbetapir (**1e**),[11−13] [^{18}F]BF228 (**1f**),[14] and [^{18}F]FDDNP[15] (**1g**) (Scheme 1).

Currently available ^{18}F-labeled compounds ($t_{1/2}$ = 109.7 min) are hampered by a higher unspecific binding, i.e. to white matter, as compared to their ^{11}C-labeled analogues ($t_{1/2}$ = 20.3 min). Thus, despite the high concentrations of Aβ in advanced AD cases, the tracer uptake ratios AD patients/healthy controls of [^{18}F]FDDNP, [18][F]Florbetaben, and [^{11}C]PiB in brain regions known to contain Aβ have been found to be 1.3,[15] 1.5,[9] and 2,[5,16] respectively.

Further development in the field of Aβ imaging aims at providing tracers for Aβ with improved opportunity for detection of less extensive amyloid pathology, that is, in patients that are not yet in an advanced clinical stage. Therefore, new pharmacophores suitable for ^{18}F-labeling with improved brain uptake and clearance kinetics, combined with high metabolic stability in vivo and high binding affinity to Aβ-plaques, are required for advances in the field of Aβ-targeted radiopharmaceuticals.

Recently, we reported the synthesis and evaluation of ^{11}C-labeled imidazo[2,1-b]benzothiazoles (IBTs) as a new pharmacophore for imaging Aβ.[17] Here, we report the synthesis and evaluation of a novel ^{18}F-labeled 2-(p-methylaminophenyl)-7-(2-fluoroethoxy)imidazo[2,1-b]benzothiazole ([^{18}F]IBT, [^{18}F]8). Compound **8** was compared with **1a** for binding affinity to Aβ fibrils in vitro, and [^{18}F]8 was used for the evaluation of brain uptake kinetics in Balb-C mice. Furthermore, the properties of [^{18}F]8 were investigated in an APP/PS1 transgenic mouse model of AD by means of in vivo μPET/CT, dual-tracer autoradiography, regional brain biodistribution, and immunohistochemistry.

The IBTs **3**−**8**, obtained in moderate to excellent isolated yield (35−95%) in a high purity (>95% by HPLC), were characterized by means of LC-MS and NMR. The IBT derivative **3** was synthesized by direct coupling of 6-methoxybenzo[d]-thiazol-2-amine and N-(4-(2-bromoacetyl)phenyl)acetamide **2** in ethanol at reflux temperature (Scheme 2). Compound **3** was deacetylated by treatment with 2 M NaOH at 100 °C for 30 min under microwave heating. Intermediate **4** was methylated using MeI in DMF to yield **5**. Compound **5** was demethylated by BBr₃

Scheme 1. PET Tracers Evaluated in Clinical Trials
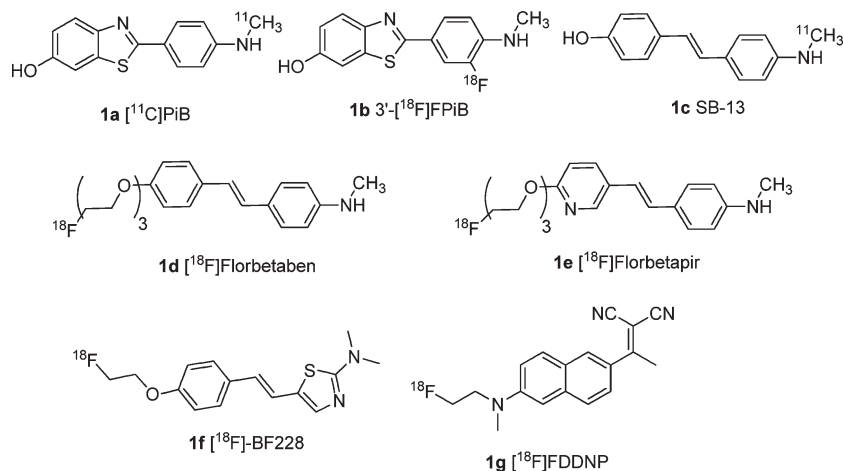
Scheme 2. Synthesis and Radiosynthesis of IBT 8[a]
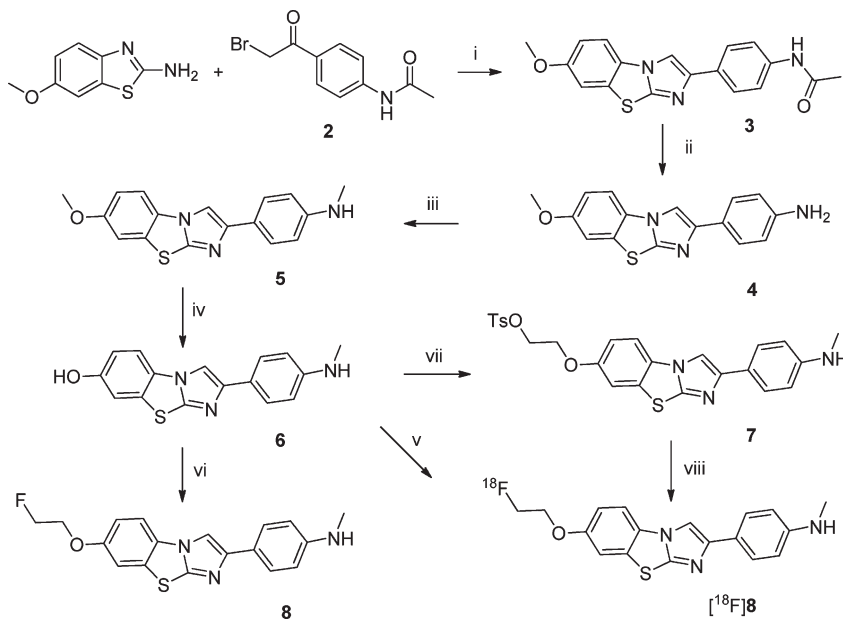
[a] Reagents and conditions: (i) EtOH, reflux, 2 h. (ii) 2 M NaOH, 100 °C, MW, 30 min. (iii) DMF, MeI, 90 °C. (iv) BBr$_3$ in CH$_2$Cl$_2$, MW, 120 °C, 30 min. (v) NaH, DMF, [^{18}F]FEtTs, 90 °C, 5 min. (vi) NaH in DMF, F(CH$_2$)$_2$Br, 80 °C, 15 min. (vii) K$_2$CO$_3$ in DMF, ethylene glycol ditosylate, 100 °C, 15 min. (viii) DMF:CH$_3$CN (1:5), [K$^+$/2.2.2]^{18}F$^-$, 120 °C, 20 min.

in CH$_2$Cl$_2$ using microwave irradiation at 120 °C for 30 min to yield **6**.

The IBT scaffold is an electron-rich heteroaromatic system with a lipophilicity value[17] suitable for in vivo imaging of targets in the brain. A further advantage is the opportunity of introducing the ^{18}F-label by means of an ^{18}F-fluoroalkyl group connected to the phenolic oxygen. In this study, compound **6** was directly reacted with F(CH$_2$)$_2$Br to yield **8** and also with ethylene glycol ditosylate to yield the precursor for one-step radiofluorination (**7**) in DMF. For the radiosynthesis, **7** was reacted with [K$^+$/2.2.2]^{18}F$^-$ to yield [^{18}F]**8** after 20 min at 120 °C in DMF:CH$_3$CN (1:5). The one-step procedure provided [^{18}F]**8** in a moderate radiochemical yield (24 ± 5%). Alternatively, [^{18}F]**8** was prepared in a high radiochemical yield via a two-step ^{18}F-fluorination (radiochemical yield,

58 ± 4%; total synthesis time, 55 min). Both procedures provided [^{18}F]**8** in a high radiochemical (>99%) and chemical purity.

For the determination of binding affinity of **8** to Aβ, fibrils of Aβ_{1-40} and Aβ_{1-42} were prepared from the respective monomers according to a published procedure.[18] The presence of fibrils was confirmed by transmission electron microscopy at 10 and 100 μM concentration. The inhibition constants, K_i, of **8** and of **1a** versus [^{3}H]**1a** are presented in Table 1.

The brain uptake kinetics of [^{18}F]**8** was compared to that of [^{11}C]**1a** at 5 and 30 min postinjection (Figure 1) in Balb-C mice ($n \geq 4$). The measure of lipophilicity of [^{18}F]**8** was determined at pH 7.4: log $P_{oct/PBS}$ = 1.92 (n = 6).

For comparison, the key preclinical data of a currently advancing ^{18}F-labeled tracer for Aβ, [^{18}F]Florbetapir, were reportedly[13]

an in vitro binding affinity to Aβ aggregates in postmortem AD brain homogenates of 2.87 ± 0.17 nM, an initial uptake of 6.2% ID/g at 2 min pi and 1.84% ID/g at 60 min in male mice. The brain uptake kinetics measurements in Balb-C mice at 5 and 30 min pi of [^{18}F]8 and [^{11}C]1a show the desirable characteristics

Table 1. K_i Values (nM; x ± SD, n = 2) Determined for Inhibition of [^{3}H]1a Binding to Aβ Fibrils

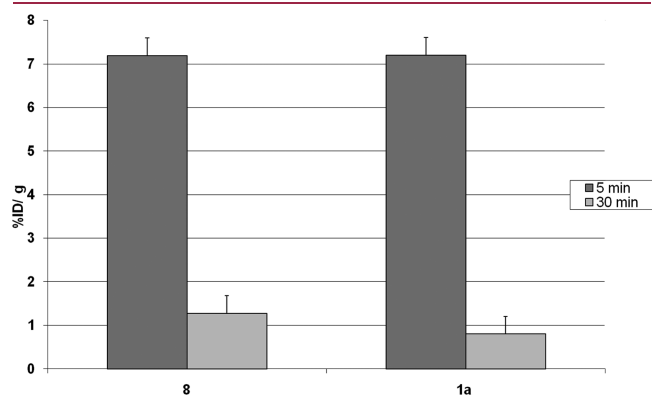| compound	8	1a
K_i Aβ_{1-40}	2.1 ± 0.8	12.0 ± 3.2
K_i Aβ_{1-42}	3.2 ± 0.6	7.7 ± 2.0

Figure 1. Brain uptake of [^{18}F]8 as compared to that of the reference [^{11}C]1a in male Balb-C mice at 5 and 30 min postinjection (mean ± SD, $n \geq 4$).

Table 2. Speciation of Radioactivity in Brain and Blood of Mice Injected with [^{18}F]8 and [^{11}C]1a (% Intact Tracer[a])

tissue	blood		brain	
	10 min	30 min	10 min	30 min
[^{18}F]8	12 ± 3	5 ± 4	92 ± 4	88 ± 6
[^{11}C]1a	20 ± 5	11 ± 2	96 ± 1	92 ± 3

[a] The extraction efficiency from the blood and brain homogenate samples was 64−95%.

for an in vivo amyloid imaging agent with an excellent initial brain uptake and rapid clearance properties.

The metabolic stabilities of [^{18}F]8 and [^{11}C]1a from in vivo experiments with Balb-C mice at 10 and 30 min pi in samples of blood and brain tissue were determined as reported elsewhere,[17,19] and the results are given in Table 2.

In vivo Aβ imaging with [^{18}F]8 in Tg mice and cross-confirmation of its imaging properties with ex vivo experiments were performed by employing homozygous animals of the APP/PS1 AD mouse model.[20] A multimodal approach was followed, including μPET/CT, ex vivo regional brain biodistribution, and dual-tracer digital autoradiography. For the PET studies, Tg animals (24.0 ± 0.4 months old; body weight, 34.5 ± 3.6 g; n = 7) were injected with a single bolus of [^{18}F]8 (11.7 ± 4.1 MBq). Age-matched C57B6/J (25 ± 2 months old; body weight, 34.8 ± 3.0 g; n = 3) were used as controls and received a single bolus injection of [^{18}F]8 (11.5 ± 3.4 MBq). The PET images (Figure 2) were generated as summed frames from 36 to 45 min pi. To obtain the anatomical reference, the CT image obtained in the PET/CT sequence was overlaid with a cerebral MRI template of an age-, gender-, and weight-matched Tg/control mouse (Figure 2).

The brain uptake kinetics in Tg animals and controls as measured by means of μPET are presented in Figure 3A. The time−radioactivity curves (TACs) from whole cortex and cerebellum and the cortex/cerebellum ratio curves in Tg and C57BL/6J control mice were calculated (Figure 3B).

For the multimodal analysis, a 25 months old Tg mouse was coinjected with a mixture of 13.5 MBq [^{18}F]8 and 4.0 MBq [^{3}H]1a into a tail vein and first scanned with a Siemens Inveon μPET/CT for 45 min in list mode. The control (28 months old) mouse received a mixture of 10.0 MBq [^{18}F]8 and 3.7 MBq [^{3}H]1a. Animals were killed at 45 min postinjection. Analysis of the data from dual-label autoradiography (tritium and fluorine-18) and brain biodistribution verified the cortical uptake of [^{18}F]8 seen in the PET studies and also that the uptake of [^{18}F]8 represents a true binding of [^{18}F]8 to cortical Aβ plaques. Furthermore, the binding profile of fluorine-18 autoradiography channels is consistent with that of 1a (Figure 4) as well as with that of the results from Aβ immunohistochemistry (IHC).

On the basis of the results from μPET/CT and ex vivo experiments in this Tg mouse model, we conclude that [^{18}F]8 has a specific binding to Aβ plaques in hippocampal and cortical
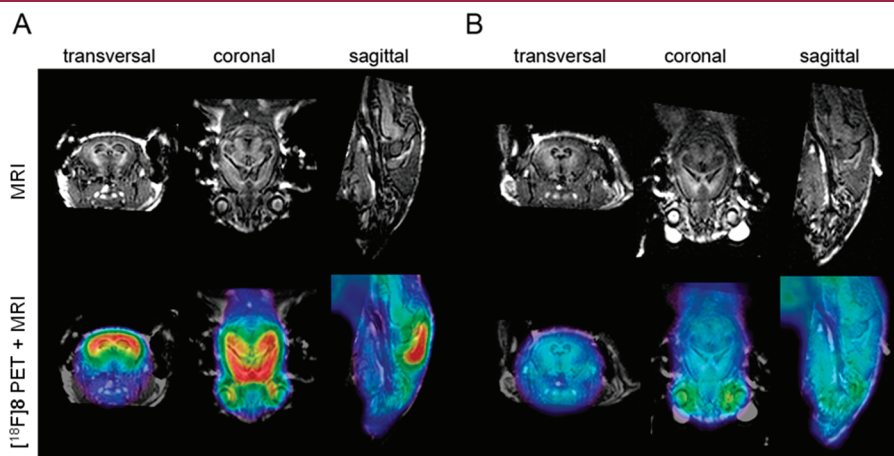

Figure 2. Orthogonal μPET images superimposed onto a MRI template. The PET signal represents the summed frames 36−45 min postinjection of [^{18}F]8 in (A) Tg and (B) control (coregistered μPET images of all animals in each experimental group were summed to generate these images).
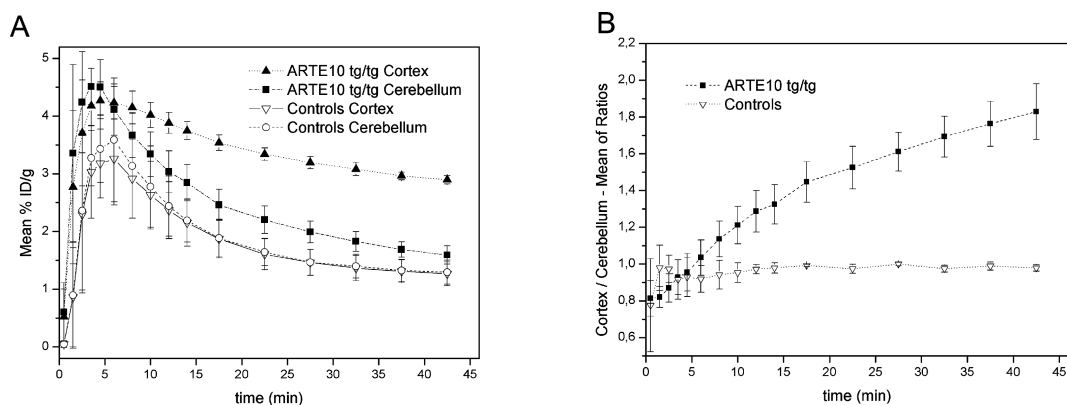
Figure 3. (A) μPET mean TACs from cortical and cerebellar VOIs in Tg ($n = 7$) and control mice ($n = 3$) of $[^{18}F]$**8**. (B) Mean of ratios in Tg ($n = 7$) and control mice ($n = 3$) of $[^{18}F]$**8**.
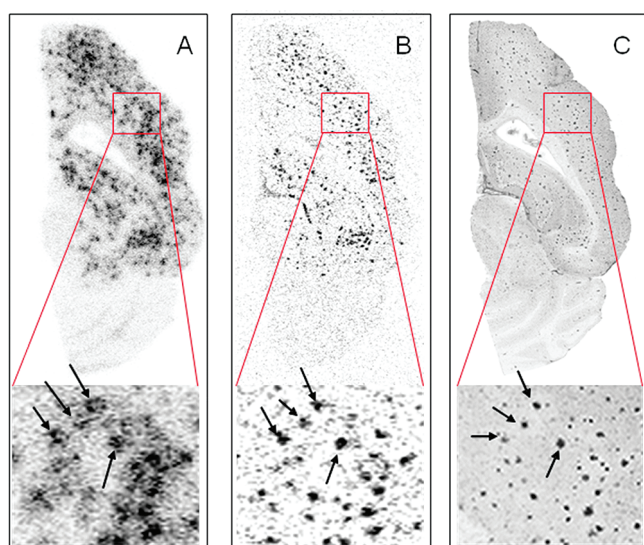

Figure 4. Ex vivo dual-tracer autoradiography of a 12 μm thick axial section of Tg mouse brain killed 45 min after coinjection of $[^{18}F]$**8** and $[^{3}H]$**1a** superimposed to the optical image. (A) Separated image of $[^{18}F]$**8** autoradiography. (B) Separated image of $[^{3}H]$**1a** autoradiography. (C) Fused IHC images of anti-Aβ_{40} and anti-Aβ_{42} (gray scale).

regions. The time–activity curves (TACs) evidenced an excellent brain uptake and clearance profile. From 5 min pi on to the end of the PET examination (45 min), an excellent differentiation of cortex and cerebellum was observed in Tg animals. In contrast, the ratio of tracer uptake in cortex relative to cerebellum in controls animals approaches unity. The potential of $[^{18}F]$**8** as a tracer for Aβ is strengthened by the results from the ex vivo regional brain biodistribution and comparison to $[^{3}H]$**1a** in dual-tracer autoradiography experiments. It was confirmed that $[^{18}F]$**8** and $[^{3}H]$**1a** bind in a similar manner to brain of APP/PS1 Tg mice. A PET study of the performance of $[^{18}F]$**8** in a younger cohort of Tg mice is currently in progress.

This proof of concept study demonstrates that the imidazo-[2,1-*b*]benzothiazole $[^{18}F]$**8** allows high-contrast imaging of Aβ in an APP/PS1 mouse model of AD by means of μPET. The favorable properties of an efficient and rapid ^{18}F-labeling combined with an excellent brain entry/clearance kinetics as well as a high affinity for the amyloid-β plaques and high in vivo stability justify the further evaluation of this compound for the detection of amyloid plaques in the living brain at an early stage of the disease.

■ ASSOCIATED CONTENT

Ⓢ Supporting Information. Full experimental details for compounds synthesized, procedures for radiosynthesis, log $P_{oct/PBS}$ measurements, description of assays, metabolite analyses, HPLC purity tests, animal studies, PET imaging, and ex vivo evaluation of control mouse. This material is available free of charge via the Internet at http://pubs.acs.org.

■ AUTHOR INFORMATION

Corresponding Authors
*Tel: +49 89 4140-6340. Fax: +49 89 4140-6493. E-mail: b.yousefi@tum.de (B.H.Y.). Tel: +49 89 4140-4586. Fax: +49 89 4140-4841. E-mail: G.Henriksen@lrz.tum.de (G.H.).

■ ACKNOWLEDGMENT

■ REFERENCES

(1) Selkoe, D. J. Toward a comprehensive theory for Alzheimer's disease. Hypothesis: Alzheimer's disease is caused by the cerebral accumulation and cytotoxicity of amyloid beta-protein. *Ann. N.Y. Acad. Sci.* **2000**, *924*, 17–25.

(2) Klunk, W. E. Biological markers of Alzheimer's disease. *Neurobiol. Aging* **1998**, *19* (2), 145–147.

(3) Selkoe, D. J. Alzheimer's disease: Genes, proteins, and therapy. *Physiol. Rev.* **2001**, *81* (2), 741–766.

676

dx.doi.org/10.1021/ml200123w |*ACS Med. Chem. Lett.* 2011, 2, 673–677

(4) Selkoe, D. J. Imaging Alzheimer's amyloid. *Nat. Biotechnol.* **2000**, *18* (8), 823–824.

(5) Klunk, W. E.; Engler, H.; Nordberg, A.; Wang, Y.; Blomqvist, G.; Holt, D. P.; Bergstrom, M.; Savitcheva, I.; Huang, G. F.; Estrada, S.; Ausen, B.; Debnath, M. L.; Barletta, J.; Price, J. C.; Sandell, J.; Lopresti, B. J.; Wall, A.; Koivisto, P.; Antoni, G.; Mathis, C. A.; Langstrom, B. Imaging brain amyloid in Alzheimer's disease with Pittsburgh Compound-B. *Ann. Neurol.* **2004**, *55*, 306–319.

(6) Koole, M.; Lewis, D. M.; Buckley, C.; Nelissen, N.; Vandenbulcke, M.; Brooks, D. J.; Vandenberghe, R.; Laere, K. V. Whole-body biodistribution and radiation dosimetry of ^{18}F-GE067: A radioligand for in vivo brain amyloid imaging. *J. Nucl. Med.* **2009**, *50*, 818–822.

(7) Nelissen, N.; Laere, K. V.; Thurfjell, L.; Owenius, R.; Vandenbulcke, M.; Koole, M.; Bormans, G.; Brooks, D. J.; Vandenberghe, R. Phase 1 Study of the Pittsburgh Compound B Derivative ^{18}F-Flutemetamol in Healthy Volunteers and Patients with Probable Alzheimer Disease. *J. Nucl. Med.* **2009**, *50*, 1251–1259.

(8) Henriksen, G.; Yousefi, B. H.; Drzezga, A.; Wester, H.-J. Development and evaluation of compounds for imaging of beta-amyloid plaque by means of positron emission tomography. *Eur. J. Nucl. Med. Mol. Imaging* **2008**, *35* (Suppl. 1), S75–S81.

(9) Rowe, C. C.; Ackerman, U.; Browne, W.; Mulligan, R.; Pike, K. L.; O'Keefe, G.; Tochon-Danguy, H.; Chan, G.; Berlangieri, S. U.; Jones, G.; Dickinson-Rowe, K. L.; Kung, H. P.; Zhang, W.; Kung, M. P.; Skovronsky, D.; Dyrks, T.; Holl, G.; Krause, S.; Friebe, M.; Lehman, L.; Lindemann, S.; Dinkelborg, L. M.; Masters, C. L.; Villemagne, V. L. Imaging of amyloid beta in Alzheimer's disease with ^{18}F-BAY94—9172, a novel PET tracer: proof of mechanism. *Lancet Neurol.* **2008**, *7* (2), 129–135.

(10) O'Keefe, G. J.; Saunder, T. H.; Ng, S.; Ackerman, U.; Tochon-Danguy, H. J.; Chan, J. G.; Gong, S.; Dyrks, T.; Lindemann, S.; Holl, G.; Dinkelborg, L.; Villemagne, V.; Rowe, C. C. Radiation Dosimetry of β-Amyloid Tracers ^{11}C-PiB and ^{18}F-BAY94—9172. *J. Nucl. Med.* **2009**, *50*, 309–315.

(11) Wong, D. F.; Rosenberg, P. B.; Zhou, Y.; Kumar, A.; Raymont, V.; Ravert, H. T.; Dannals, R. F.; Nandi, A.; Brai1, J. B.; Ye, W.; Hilton, J.; Lyketsos, C.; Kung, H. F.; Joshi, A. D.; Skovronsky, D. M.; Pontecorvo, M. J. In Vivo Imaging of Amyloid Deposition in Alzheimer Disease Using the Radioligand 18F-AV-45 (Flobetapir F 18). *J. Nucl. Med.* **2010**, *51*, 913–920.

(12) Kung, H. F.; Choi, S. R.; Qu, W.; Zhang, W.; Skovronsky, D. ^{18}F Stilbenes and Styrylpyridines for PET Imaging of Aβ Plaques in Alzheimer's Disease: A Miniperspective. *J. Med. Chem.* **2010**, *53*, 933–941.

(13) Choi, S. R.; Golding, G.; Zhuang, Z.; Zhang, W.; Lim, N.; Hefti, F.; Benedum, T. E.; Kilbourn, M. R.; Skovronsky, D.; Kung, H. F. Preclinical Properties of 18F-AV-45: A PET Agent for Aβ Plaques in the Brain. *J. Nucl. Med.* **2009**, *50*, 1887–1894.

(14) Kudo, Y.; Okamura, N.; Furumoto, S.; Tashiro, M.; Furukawa, K.; Maruyama, M.; Itoh, M.; Iwata, R.; Yanai, K.; Arai, H. 2-(2-[2-Dimethylaminothiazol-5-yl]ethenyl)-6- (2-[fluoro]ethoxy)benzoxazole: A novel PET agent for *in vivo* detection of dense amyloid plaques in Alzheimer's disease patients. *J. Nucl. Med.* **2007**, *48*, 553–561.

(15) Thompson, P. W.; Ye, L.; Morgenstern, J. L.; Sue, L.; Beach, T. G.; Judd, D. J.; Shipley, N. J.; Libri, V.; Lockhart, A. Interaction of the amyloid imaging tracer FDDNP with hallmark Alzheimer's disease pathologies. *J. Neurochem.* **2009**, *109*, 623–630.

(16) Pike, K. E.; Savage, G.; Villemagne, V. L.; Ng, S.; Moss, S. A.; Maruff, P.; Mathis, C. A.; Klunk, W. E.; Masters, C. L.; Rowe, C. C. Beta-amyloid imaging and memory in non-demented individuals: Evidence for preclinical Alzheimer's disease. *Brain* **2007**, *130*, 2837–2844.

(17) Yousefi, B. H.; Manook, A.; Drzezga, A.; von Reutern, B.; Schwaiger, M.; Wester, H.-J.; Henriksen, G. Synthesis and Evaluation of ^{11}C-labeled Imidazo[2,1-*b*]benzothiazoles (IBTs) as PET tracers for Imaging β-Amyloid Plaques in Alzheimer's Disease. *J. Med. Chem.* **2011**, *54*, 949–956.

(18) Lockhart, A.; Ye, L.; Judd, D. B.; Merritt, A. T.; Lowe, P. N.; Morgenstern, J. L.; Hong, G.; Gee, A. D.; Brown, J. Evidence for the presence of three distinct binding sites for the thioflavin T class of Alzheimer's disease PET imaging agents on beta-amyloid peptide fibrils. *J. Biol. Chem.* **2005**, *280*, 7677–7684.

(19) Henriksen, G.; Hauser, A. I.; Westwell, A. D.; Yousefi, B. H.; Schwaiger, M.; Drzezga, A.; Wester, H.-J. Metabolically stabilized benzothiazoles for imaging of amyloid plaques. *J. Med. Chem.* **2007**, *50*, 1087–1089.

(20) Willuweit, A.; Velden, J.; Godemann, R.; Manook, A.; Jetzek, F.; Tintrup, H.; Kauselmann, G.; Zevnik, B.; Henriksen, G.; Drzezga, A.; Pohlner, J.; Schoor, M.; Kemp, J. A.; von der Kammer, H. Early-Onset and Robust Amyloid Pathology in a New Homozygous Mouse Model of Alzheimer's Disease. *PLoS ONE* **2009**, *4* (11), e7931.